J. of Basic Sciences, Cheju Nat'l Univ.
12(1), 35~39, 1999

기초과학연구 제주대학교
12(1), 35~39, 1999

McIntyre Strong Absorption Model Analysis for π^- + ^{40}Ca and K^- + ^{40}Ca Elastic Scatterigs at 800 MeV/c

Yong Joo Kim and Nam Gyu Hyun
Department of Physics, Cheju National University, Cheju 690-756

Dong Shik Kang
Department of Science Education, Cheju National Univeristy, Cheju 690-756

The elastic scatterings of 800 MeV/c negative pion and kaon from ^{40}Ca nucleus have been analyzed within the framework of McIntyre strong absorption model. Reasonable agreements between the calculated results and observed data are obtained in both cases. The near- and far-side decompositions of elastic cross section have been also performed by following the Fuller's formalism. An expression of optical potential by inversion has been derived and its results are presented.

I. INTRODUCTION

For many year, the McIntyre strong absorption model (SAM) [1] is known as a useful tool to describe the heavy ion elastic scattering. This model has been proved to give good fits to the nucleus-nucleus elastic scattering data over a wide energy range. Mermaz [2,3] has successfully used the McIntyre parametrization to fit the elastic scattering data of ^{12}C+^{12}C and ^{16}O scatterings on ^{12}C, ^{40}Ca, ^{90}Zr and ^{208}Pb targets. Elastic scattering data for ^{12}C+^{12}C and ^{12}C+^{208}Pb systems at $E_{\rm lab}$=1449 and 2400 MeV have been also fitted well by Mermaz *et al.* [4] using this model. Very precise measurements of the cross sections of 800 MeV/c negative charged pion and kaon scattered from ^{40}Ca nucleus were performed [5,6] at Brookhaven National Laboratory. The elastic scattering cross sections data were analyzed within the framework of the first-order optical model. Recently, Choudhury [7,8] analyzed these data by using a phenomenological model based on Frahn-Venter SAM and Ericson SAM for π^- + ^{40}Ca and K^- + ^{40}Ca systems, respectively. A reasonable agreements between the calculated results and the experimental data were obtained in both cases.

On the other hand, several inversion problems of evaluating optical potential from the parametrized phase shift were studied [9,10]. Fayyad *et al.* [9] have shown by solving the inversion problem at high energies that the fundamental McIntyre parametrization of the S-matrix, for heavy ion collision, could correspond to a Woods-Saxon type optical model potential. The parameters of such a Woods-Saxon potential were found to relate directly to the corresponding parameters of the McIntyre parametrization. Eldebawi and Simbel [10] used the simple Ericson parametrization of the phase shifts to analyze the elastic scattering of ^{12}C+^{12}C at $E_{\rm lab}$=139.5 ~ 2400 MeV and of ^{16}O+^{16}O at $E_{\rm lab}$=608 MeV and applied the Glauber approximation to evaluate the corresponding optical potential. Ahmad *et al* [11]. have studied the effect of the non-eikonal corrections on the determination of heavy ion optical potential from the diffraction model phase shifts at intermediate energies.

In previous papers [12-14], a semiclassical phase shift analysis based on McIntyre SAM was presented. It was applied satisfactorily to the so-called Fresnel patterns ^{12}C+^{90}Zr and ^{12}C+^{208}Pb elastic scatterings at $E_{\rm lab}/A$=35 MeV/nucleon [12]. In recent, elastic scattering data of K^+ + ^{12}C and K^+ + ^{40}Ca systems at 800 MeV/c were reproduced and inverse potentials were predicted [15] in the framework of McIntyre SAM. A phase shift analysis and first-order eikonal correction to optical potential by inversion for ^{16}O + ^{28}Si elastic scattering were presented [16].

In this paper, we present a McIntyre SAM analysis of elastic scattering data for 800 MeV/c negative charged pion and kaon from the ^{40}Ca nucleus. Furthermore, optical potentials will be obtained by using the inversion procedure. In Section II, we present the scattering amplitude and relevant formalism for an expression of optical potential by inversion based on the McIntyre parametrization. Finally, we present and discuss the results of our calculation and conclusions in Sec. III.

II. SCATTERING AMPLITUDE AND POTENTIAL BY INVERSION

A. Scattering Amplitude

The elastic scattering amplitude for spin-zero particle via Coulomb and short-range central force is given by

$$f(\theta) = f_{\rm R}(\theta) + \frac{1}{ik}\sum_{l=0}^{\infty}\left(l+\frac{1}{2}\right)\exp(2i\sigma_l)(S_l^{\rm N}-1)P_l(\cos\theta) \tag{1}$$

Here $f_{\rm R}(\theta)$ is the usual Rutherford scattering amplitude, σ_l the Coulomb phase shifts. In the above equation, k is

the meson wave number in the center of mass coordinate system and is given by

$$k = \frac{m_N}{\hbar}\left[\frac{(E_M^2/c)^2 - m_M^2c^2}{m_M^2 + m_N^2 + 2m_N E_M/c^2}\right]^{1/2} \quad (2)$$

where m_M and m_N are the meson and nuclear rest mass, respectively. E_M is the total meson energy in the laboratory system. In Eq. (1), S_l^N denotes the nuclear scattering matrix by the following formula

$$S_l^N = A_l \exp(2i\delta_R) = \exp\{2i[\delta_R(l) + i\delta_I(l)]\}. \quad (3)$$

In this work, we use the McIntyre parametrization of the S-matrix. The McIntyre parametrization [1] is expressed for the phase shift of a nuclear S-matrix, S_l^N, as

$$\delta_R(l) = \mu\{1 + \exp[(l - \Lambda_1)/\Delta_1)]\}^{-1} \quad (4)$$

and for the modulus of S_l^N as

$$A_l = |S_l^N| = \{1 + \exp[(\Lambda_2 - l)/\Delta_2]\}^{-1}. \quad (5)$$

In the above two equations (4) and (5), there are five adjustable parameters available for fitting the cross section data: Λ_1, Λ_2, Δ_1, Δ_2 and μ. The two grazing angular momneta Λ_1 and Λ_2 are related semiclassically to the interaction radius of the colliding nuclei. While the corresponding widths Δ_1 and Δ_2 are related to the thickness of the region in which the nuclear interaction between the colliding nuclei takes place without destruction of the identity of either of the nuclei. The remaining parameter, μ, is required to introduce the strength of the nuclear phase shift.

The real and imaginary parts of nuclear phase shift can further be written as

$$\delta_R(b) = \frac{\mu}{1 + \exp[(b - b_0')/d']} \quad (6)$$

and

$$\delta_I(b) = \frac{1}{2}\ln\left[1 + \exp\left(\frac{b_0 - b}{d}\right)\right] \quad (7)$$

where b, b_0 and b_0' are the impact parameters normally given by $kb = l + 1/2$, $kb_0 = \Lambda_2 + 1/2$ and $kb_0' = \Lambda_1 + 1/2$, respectively. The diffusivity quantities d and d' are given by $d = \Delta_2/k$ and $d' = \Delta_1/k$.

B. Optical Potential by Inversion

Using the relation between nuclear phase shift and optical potential [9], one can now obtain the expressions for the nuclear phase shift

$$\delta(b) = -\frac{k}{2E}\int_b^\infty \frac{r(V(r) + iW(r))}{\sqrt{r^2 - b^2}}\,dr = \delta_R(b) + i\delta_I(b) \quad (8)$$

where the real and imaginary parts of the nuclear phase shift are

$$\delta_R(b) = -\frac{k}{2E}\int_b^\infty \frac{rV(r)}{\sqrt{r^2 - b^2}}\,dr \quad (9)$$

and

$$\delta_I(b) = -\frac{k}{2E}\int_b^\infty \frac{rW(r)}{\sqrt{r^2 - b^2}}\,dr. \quad (10)$$

The above Eqs. (9) and (10) are of Abel's type and the corresponding inverse eikonal relations for the real and imaginary parts of optical potential are given by

$$V(r) = \frac{4E}{k\pi}\frac{1}{r}\frac{d}{dr}\int_r^\infty \frac{\delta_R(b)}{\sqrt{b^2 - r^2}}\,b\,db \quad (11)$$

and

$$W(r) = \frac{4E}{k\pi}\frac{1}{r}\frac{d}{dr}\int_r^\infty \frac{\delta_I(b)}{\sqrt{b^2 - r^2}}\,b\,db. \quad (12)$$

Replacing $b = \sqrt{r^2 + u^2}$, we can derive the following optical potential form

$$V(r) = -\frac{4E\mu}{k\pi d'}\int_0^\infty du\frac{1}{\sqrt{r^2 + u^2}}\frac{\exp\left(\frac{\sqrt{r^2+u^2} - b_0'}{d'}\right)}{\left[1 + \exp\left(\frac{\sqrt{r^2+u^2} - b_0'}{d'}\right)\right]^2} \quad (13)$$

and

$$W(r) = -\frac{2E}{k\pi d}\int_0^\infty du\frac{1}{\sqrt{r^2 + u^2}}\frac{1}{1 + \exp\left(\frac{\sqrt{r^2+u^2} - b_0}{d}\right)}. \quad (14)$$

The above Eqs. (13) and (14) can be calculated numerically by using the five parameters of McIntyre phase shift.

III. RESULTS AND CONCLUSIONS

The elastic differential cross sections are obtained by using partial wave sum, Eq. (1) and McIntyre phase shifts, Eqs. (4)-(5). The elastic scattering angular distributions for π^- + ^{40}Ca and K^- + ^{40}Ca systems at 800 MeV/c are presented in Fig. 1. The fits are excellent and the corresponding parameters are given in table I. In Fig. 1, the calculated differential cross sections of McIntyre SAM are compared with the results of the phenomenological model [7,8] based on Frahn-Venter SAM, Ericson SAM and with the observed data [5,6] for π^- + ^{40}Ca and K^- + ^{40}Ca systems at 800 MeV/c. In this figure, the solid and dashed curves represent the cross sections of the McIntyre SAM and the ones of the phenomenological model, respectively.It is seen that the agreements of our model with the observed data are satisfactorily good

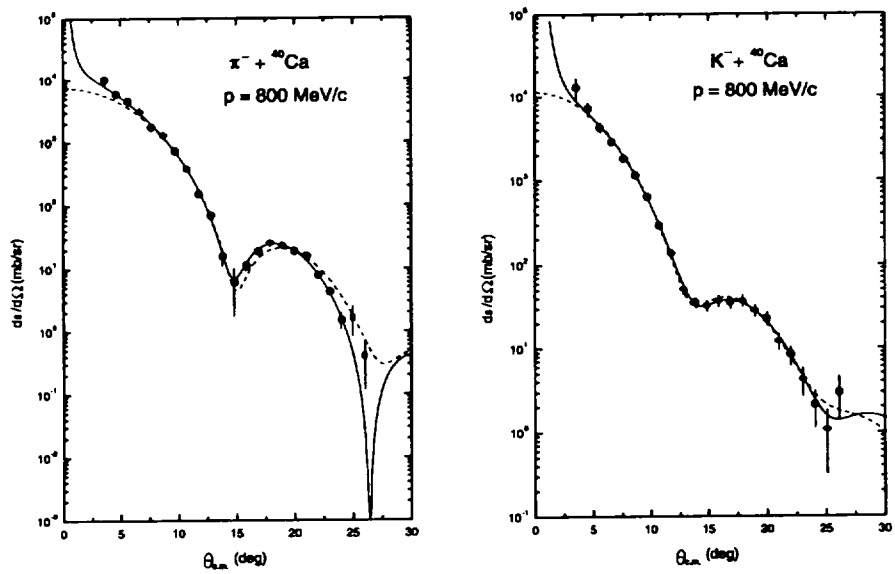

FIG. 1. Elastic scattering angular distributions for $\pi^- + {}^{40}Ca$ and $K^- + {}^{40}Ca$ elastic scatterings at 800 MeV/c. The solid circles denote the observed data taken from Ref. [5,6]. The solid curves are the our calculated results using the McIntyre SAM. The dashed curves are the Frahn-Venter SAM for $\pi^- + {}^{40}Ca$ and Ericson SAM for $K^+ + {}^{40}Ca$ elastic scatterings, respectively.

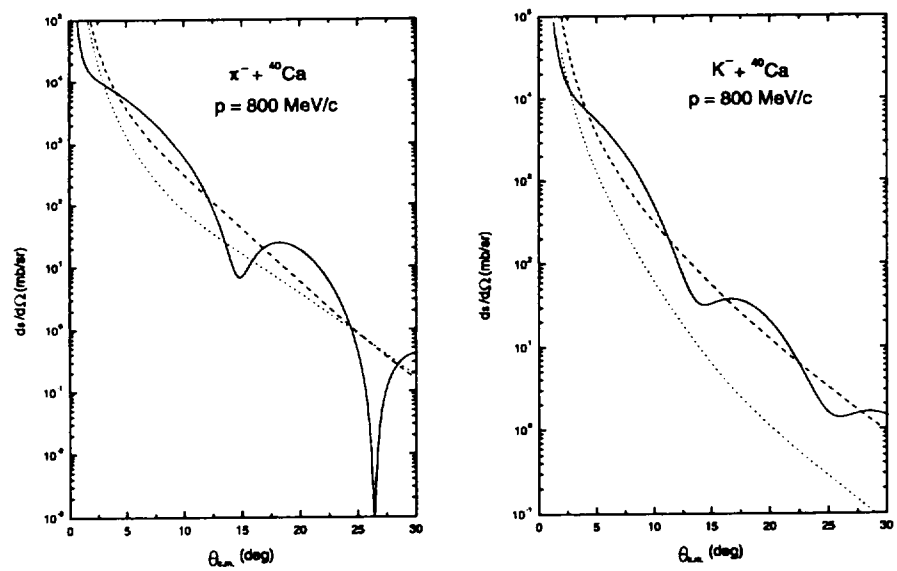

FIG. 2. Differential cross sections (solid curves), near-side contributions (dotted curves), and far-side contributions (dashed curves) following Fuller's formalism [17] by using McIntyre parametrization of S-matrix.

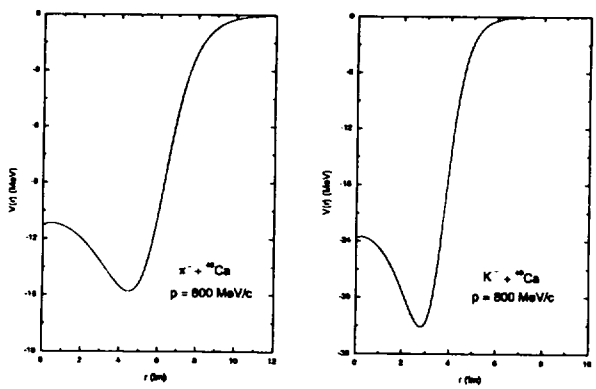

FIG. 3. The real parts of the optical potential for π^-+^{40}Ca and K$^-$+^{40}Ca elastic scattering at 800 MeV/c.

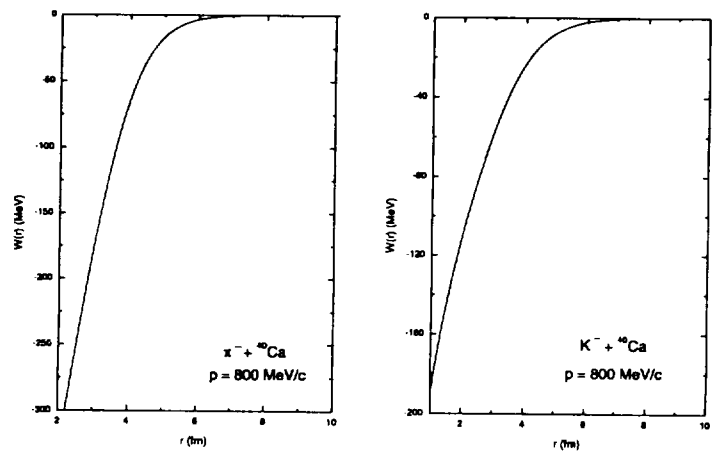

FIG. 4. The imaginary parts of the optical potential for π^-+^{40}Ca and K$^-$+^{40}Ca elastic scattering at 800 MeV/c.

TABLE I. Input values of McIntyre strong absorption model for π^- + ^{40}Ca and K$^-$ + ^{40}Ca elastic scatterings at 800 MeV/c.

System	$r_{1/2}$(fm)	d(fm)	μ	$r_{\rm ph}$(fm)	$d_{\rm ph}$(fm)	Λ_1	Δ_1	Λ_2	Δ_2
π^- + ^{40}Ca	1.045	0.658	0.147	1.656	0.907	22.502	3.600	14.209	2.611
K$^-$ + ^{40}Ca	0.996	0.810	0.444	0.987	0.505	13.442	1.998	13.564	3.204

TABLE II. Analysis results from McIntyre strong absorption model for π^- + ^{40}Ca and K$^-$ + ^{40}Ca elastic scatterings at 800 MeV/c.

System	θ_g(deg)	$\theta_{N.R}$(deg)	R_{SAR}(fm)	$\sigma_{R,1/2}$(mb)	σ_R(mb)	χ^2/N
π^- + ^{40}Ca	-0.209°	-1.302°	4.286	577	630	1.64
K$^-$ + ^{40}Ca	-0.770°	-7.145°	4.270	573	646	0.26

in both cases compared to the results of the phenomenological model based on Franh-Venter SAM and Ericson SAM. In table II, $\theta_g = 2\ \mathrm{ArcTan}(\eta/\Lambda_2)$ is the grazing angle. And $\theta_{N.R}$ is the nuclear rainbow angle obtained from the deflection function $\theta_l = 2(\sigma_l + \delta_R)/dl$. It can be noticed in table II that the nuclear rainbows exist in both systems $\pi^- + {}^{40}Ca$ and $K^- + {}^{40}Ca$ at 800 MeV/c. The strong absorption radius R_{SAR} in table II is defined as the distance for which $|S_l^N|^2 = 1/2$, i.e. the distance where the incident particle has the same probability to be absorbed as to be reflected. We can see that the strong absorption radius R_{SAR} gives a proper measure of the reaction cross section in terms of $\sigma_{R,1/2} = \pi R_{SAR}^2$.

The near- and far-side decompositions [17] of the scattering amplitudes with the McIntyre parametrization of S-matrix were also performed by replacing the associated Legendre polynominals $P_{lm}(\cos\theta)$ by

$$Q_{lm}^{\pm}(\cos\theta) = \frac{1}{2}\left(P_{lm}(\cos\theta) \mp \frac{2}{\pi}Q_{lm}(\cos\theta)\right),$$

where Q_{lm} is a Legendre function of the second kind. The contributions of the near- and far-side components to elastic scattering cross sections are shown in Fig. 2 along with the total differential cross section. The total differential cross section is not just a sum of the near- and far- side cross sections but contains the interference between near- and far-side amplitudes as seen in Fig. 2. The oscillation features of the angular distributions for $\pi^- + {}^{40}Ca$ and $K^- + {}^{40}Ca$ systems at 800 MeV/c are mainly due to interferences between near- and far-side amplitudes. It is also noted that the far-side amplitudes in these systems dominate as a whole.

Our method to calculate the inversion potential is made a direct application of phase shift to inverse eikonal relation, and the expressions of inverse potential, Eqs(13) and (14), were obtained as an integral forms in terms of McIntyre phase shift parameters. The integration in Eqs. (13) and (14) has been performed numerically using the McIntyre parameters listed in table 1. Figures 3-4 show the real and imaginary parts of optical potential. In these figures, we can find that imaginary parts of the optical potential are extraordinary deep compared to the real ones of optical potentials.

In this paper, we have presented a McIntyre strong absorption model analysis of negative charged pion and kaon scattering on ^{40}Ca. We have found that calculated results of the McIntyre SAM are in excellent agreements with the observed data of $\pi^- + {}^{40}Ca$ and $K^- + {}^{40}Ca$ systems at 800 MeV/c. We can see that the strong absorption radius R_{SAR} gives a proper measure of the reaction cross section in terms of $\sigma_{R,1/2} = \pi R_{SAR}^2$. Through a near-side and far-side decomposition of the cross section following the Fuller's formalism [17], we have also shown that the oscillations of angular distribution in these systems are due to the interferences between the near-side and far-side amplitude. We have also found in these systems that the far-side amplitudes dominate as a whole. A new expression of the optical potential was analytically derived from the inversion procedure. We can find in this model that imaginary parts of the optical potential are extraordinary deep compared to the real ones of optical potentials.

ACKNOWLEDGMENTS

The present study was partially supported by Cheju National University Research Fund, 1999.

[1] J. A. McIntyre, K. H. Wang and L. C. Becker, Phys. Rev. **117**, 1337 (1960).
[2] M. C. Mermaz, Il Nuovo Cimento **88A**, 286 (1985).
[3] M. C. Mermaz, Z. Phys. **A321**, 613 (1985).
[4] M. C. Mermaz, B. Bonin, M. Buenerd and J. Y .Hostachy, Phys. Rev. **C34**, 1988 (1986).
[5] D.Marlow, P.D.Barnes, N.J.Colella, S.A.Dytman, R.A.Eisentein, R.Grace, P. Pile, F.Takeutchi, W.R.Wharton, S.Bart, D.Hancock, R.Hackenberg, E.Hungerford, W.Mayes, L.Pinsky, T.Williams, R.Charien, H.Palevsky and R.Sutter, Phys. Rev. **C30**, 1662 (1984).
[6] D.Marlow, P.D.Barnes, N.J.Colella, S.A.Dytman, R.A.Eisentein, R.Grace, F.Takeutchi, W.R.Wharton, S.Bart, D.Hancock, R.Hackenberg, E.Hungerford, W.Mayes, L.Pinsky, T.Williams, R.Charien, H.Palevsky and R.Sutter, Phys. Rev. **C25**, 2619 (1982).
[7] D.C.Choudhury and M.A.Scura, Phys. Rev. **C47**, 2404 (1993).
[8] D.C. Choudhury, J. Phys. **G22**, 1069 (1996).
[9] H. M. Fayyad and T. H. Rihan, Phys. Rev. **C53**, 2334 (1996).
[10] N. M. Eldebawi and M. H. Simbel, Phys. Rev. **C53**, 2973 (1996).
[11] I. Ahmad, J. H. Madani and M. A. Abulmomen, J. Phys. G: Nucl. Part. Phys. **24**, 899 (1998).
[12] M. H. Cha and Y. J. Kim, J. Phys. G: Nucl. Part. Phys. **16**, L281 (1990).
[13] M. H. Cha, B. K. Lee and Y. J. Kim, J. Korean Phys. Soc. **23**, 369 (1990).
[14] M. H. Cha, B. K. Lee K. S. Sim and Y. J. Kim, J. Korean Phys. Soc. **23**, 450 (1990).
[15] Y. J. Kim and M. H. Cha, J. Korean Phys. Soc. **34**, 339 (1999).
[16] Y. J. Kim and M. H. Cha, Int. J. Mod. Phys. **E8**, 311 (1999).
[17] R.C.Fuller, Phys. Rev. **C12**, 1561 (1975).